# Structural basis of heroin and cocaine metabolism by a promiscuous human drug-processing enzyme

Sompop Bencharit[1,2], Christopher L. Morton[3], Yu Xue[1], Philip M. Potter[3] and Matthew R. Redinbo[1,4]

Published online 7 April 2003; doi:10.1038/nsb919

**We present the first crystal structures of a human protein bound to analogs of cocaine and heroin. Human carboxylesterase 1 (hCE1) is a broad-spectrum bioscavenger that catalyzes the hydrolysis of heroin and cocaine, and the detoxification of organophosphate chemical weapons, such as sarin, soman and tabun. Crystal structures of the hCE1 glycoprotein in complex with the cocaine analog homatropine and the heroin analog naloxone provide explicit details about narcotic metabolism in humans. The hCE1 active site contains both specific and promiscuous compartments, which enable the enzyme to act on structurally distinct chemicals. A selective surface ligand-binding site regulates the trimer-hexamer equilibrium of hCE1 and allows each hCE1 monomer to bind two narcotic molecules simultaneously. The bioscavenger properties of hCE1 can likely be used to treat both narcotic overdose and chemical weapon exposure.**

Human carboxylesterase 1 (hCE1) is a serine hydrolase found in the liver, small intestine, kidney, lung, testes, heart, monocytes, macrophages and circulating plasma[1,2]. The enzyme hydrolyzes esters, amides and thioesters in a variety of chemically distinct compounds and plays a central role in the metabolism of xenobiotics, including cocaine and heroin[3,4], and clinical drugs, such as lovastatin, lidocaine and angiotensin-converting enzyme inhibitors[5–7]. hCE1 (also called egasyn) regulates the endoplasmic reticulum (ER) retention of C-reactive protein and β-glucuronidase in liver[8]. hCE1 is also being aggressively developed by the United States military as a defense against the chemical weapons sarin, soman, tabun and VX gas[9–11].

Cocaine is metabolized by three human enzymes: hCE1, intestinal CE (also termed human CE2) and serum butyrylcholinesterase (hBuChE). Although intestinal CE and hBuChE hydrolyze the larger benzoyl ester linkage on cocaine, only hCE1 hydrolyzes the methyl ester linkage to generate benzoylecgonine, the primary urinary metabolite of cocaine (Fig. 1*a*). All three enzymes hydrolyze heroin to 6-acetylmorphine[3,12–14] (Fig. 1*b*). hCE1 is also responsible for the creation of the toxic cocaine metabolite cocaethylene, formed when cocaine and alcohol are

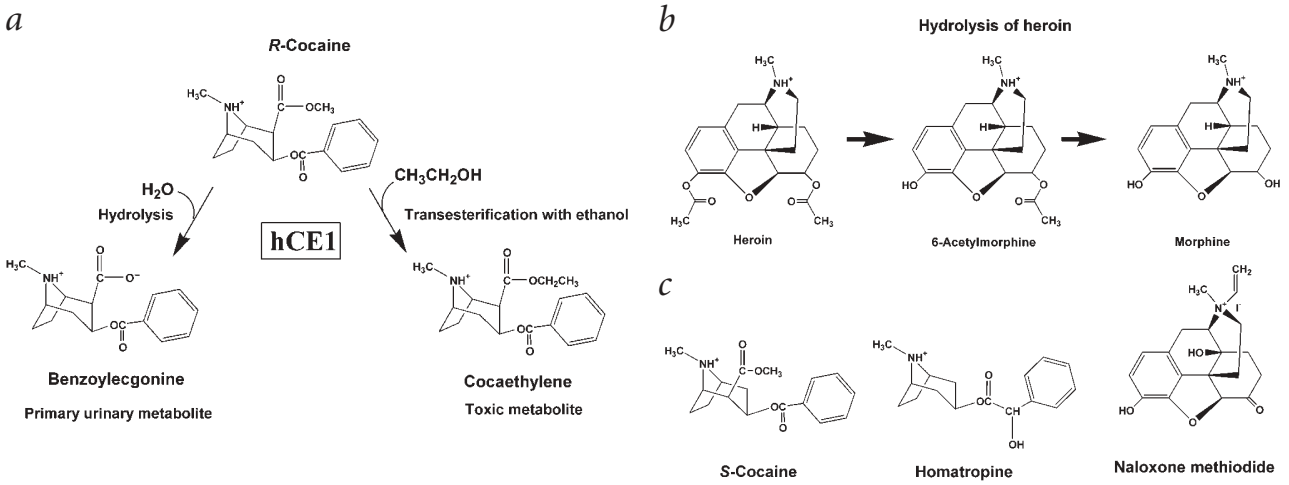


**Fig. 1** Cocaine and heroin metabolism. ***a***, The role of hCE1 in cocaine metabolism. hCE1 catalyzes the methyl ester hydrolysis of *R*-cocaine, the active stereoisomer, to benzoylecgonine. When cocaine and alcohol are abused together, hCE1 also catalyses the transesterification of cocaine to cocaethylene, a toxic metabolite with a long half-life in humans. ***b***, The role of hCE1 in the conversion of heroin to 6-acetylmorphine and morphine. ***c***, Chemical structures of *S*-cocaine, an inactive stereoisomer of cocaine, the cocaine analog homatropine and the heroin analog naloxone methiodide.

[1]Department of Chemistry, University of North Carolina at Chapel Hill, Chapel Hill, North Carolina 27599, USA. [2]School of Dentistry, University of North Carolina at Chapel Hill, Chapel Hill, North Carolina 27599, USA. [3]Department of Molecular Pharmacology, St. Jude Children's Research Hospital, Memphis, Tennessee 38105, USA. [4]Department of Biochemistry & Biophysics and the Lineberger Comprehensive Cancer Center, University of North Carolina at Chapel Hill, Chapel Hill, North Carolina 27599, USA,

Correspondence should be addressed to M.R.R. *e-mail: redinbo@unc.edu*

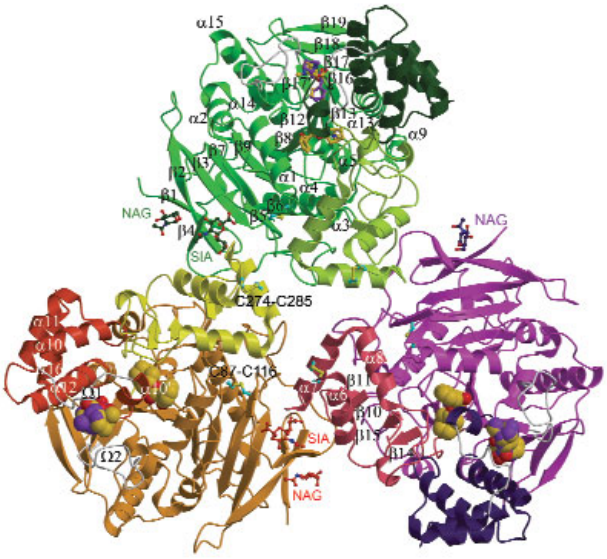


**Fig. 2** The hCE1 trimer as observed in the homatropine complex, viewed down the three-fold axis of symmetry and into the active site gorge of each molecule. Individual monomers are colored by domain: the catalytic domain (green, magenta and orange), the αβ domain (light green, pink and yellow), and the regulatory domain (dark green, purple and red). The secondary structure of the catalytic domain is labeled in the green monomer, the αβ domain in the pink-purple monomer and the regulatory domain in the orange-red monomer. The Ω loops (white) are also indicated in each monomer, and labeled in the red monomer; the disulfide linkages (Cys87-Cys116 and Cys274-Cys285) are cyan. *N*-acetylglucosamine (NAG) and sialic acid (SIA) sugar moieties are colored according to each monomer, and homatropine molecules bound at the active sites are gold. Homatropines bound at the Z site, between the Ω loops, are gold and purple. The r.m.s. deviation over Cα atoms between monomers within the homatropine complex are 0.28–0.43 Å; between monomers within naloxone complex, 0.30–0.43 Å; and between monomers of the two complexes, 0.28–0.57 Å.

abused together — a common pattern in the United States[15] (Fig. 1*a*). Cocaethylene is generated by transesterification and ethyl-ester exchange reactions, and the metabolite shows a longer half-life, higher brain/plasma distribution ratio and greater toxicity than cocaine[15]. We sought to explain the structural basis of the ability of hCE1 to act both selectively and promiscuously in metabolizing cocaine and heroin.

## Overview of hCE1 structures

Crystal structures of hCE1 in complex with the cocaine analog homatropine or the heroin analog naloxone methiodide were refined to 2.8 Å and 2.9 Å resolution, respectively (Fig. 1*c*). The homatropine complex contains two trimers in the asymmetric unit, whereas the naloxone complex contains two hexamers (Table 1). The enzyme shows an α/β-hydrolase fold consisting of a central catalytic domain and surrounding αβ and regulatory domains[16] (Fig. 2). The catalytic domain (strands β1–9, β12–13 and β16–19, and helices α1–5, α9 and α13–15) contains the serine hydrolase catalytic triad (Ser221, Glu354 and His468) at the base of the active site gorge. The αβ domain is composed of α6–8, β10–11 and β14–15, and the regulatory domain consists of α10–12, α10′ and α16. Residues 355–372, disordered and not observed in a related rabbit carboxylesterase (rCE) structure[16], form α10′ and an Ω loop[17] (Ω1) in hCE1. α10′ closes over the active site of hCE1; thus, the structures presented here provide the first views of a complete catalytic gorge of a mammalian carboxylesterase. Similarly, residues 452–469, also disordered in rCE, form β17′ and another Ω loop (Ω2) within the main catalytic domain of hCE1. These newly observed Ω1 and Ω2 loops interdigitate and form critical packing interactions in the hCE1 hexamer (described below). hCE1 shares 81% sequence identity and 0.68 Å r.m.s. deviation over Cα positions with rCE, and 30% sequence identity and 1.2 Å r.m.s. deviation over Cα positions with human acetylcholinesterase[16,18]. The presence in hCE1 of α10′, Ω1, Ω2 and β17′, as well as the lack of an *N*-linked glycosylation site at residue 390, represent the most significant structural differences between hCE1 and rCE.

The entrance to the substrate-binding gorge of each hCE1 monomer is framed by α-helices from all three domains (α1, α8, α10′ and α14) and surrounded by both polar and non-polar residues, including Asp90, Ala93, Leu294, Lys302, Leu304, Leu363 and Met364 (Fig. 3*a*). Some residues in this region (for example, Leu304 and Leu363) show structural flexibility and shift in position by up to 2 Å between monomers within the same complex. The catalytic triad (Ser221, Glu354 and His468), which resides at the base of the substrate-binding gorge, is aligned in a manner typical of serine esterases. The substrate-binding gorge contains a large, flexible pocket on one side of Ser221 and a small, rigid pocket on the opposite side (Flex and Rig, respectively; Fig. 3*a*). The rigid pocket, adjacent to the oxyanion hole defined by Gly142 and Gly143, is lined by Leu96, Leu97, Leu100, Leu358 and Phe101. When individual monomers in the homatropine and naloxone complexes are compared, the side chain atoms of these residues shift in position by an average of 1.0 Å and maximally by 1.8 Å. The flexible pocket is lined by Leu255, Leu304, Leu318, Leu363, Leu388, Thr252, Met364, Met425 and Phe426. The side chain atoms of these residues, in contrast to those in the rigid pocket, shift in position (between individual monomers) by an average of 1.9 Å and maximally by 4.2 Å. Thus, the larger pocket is more flexible than the smaller pocket. This larger, flexible compartment also lies adjacent to the 'side door' secondary pore, which has been proposed to shuttle small compounds into and out of the active site of carboxylesterases[16] and may be critical to the transesterification reactions catalyzed by hCE1.

## Cocaine metabolism by hCE1

The cocaine analog homatropine was placed into clear simulated annealing omit electron density in the substrate-binding pocket of hCE1 (Fig. 3*b,d,e*). The site on homatropine where the methyl ester linkage would exist on the *R*-stereoisomer of cocaine is oriented toward the small, rigid pocket, while the benzoyl and tropine groups of homatropine pack within the large, flexible pocket of the enzyme (Fig. 3*b,d–f*). An equimolar mix of *R*- and *S*-homatropine was used in crystallization, and, although both stereoisomers bind to the second surface ligand-binding site on hCE1 (the 'Z site', see below), only the *R*-stereoisomer is observed in the active site of the enzyme. The binding of homatropine to hCE1 reveals how the enzyme is site- and stereospecific for hydrolysis and transesterification of the methyl ester linkage on *R*-cocaine[4]. We docked *R*-cocaine into the active site using the tropine ring of homatropine as a guide and found that the methyl ester linkage of *R*-cocaine is aligned for nucleophilic attack by Ser221 (2.6 Å away) and the transition state is stabilized *via* the amide nitrogens of Gly142 and Gly143 (3.9 and 3.1 Å away, respectively) that form the oxyanion hole (Fig. 3*b,f*). The docking of *S*-cocaine (Fig. 1*c*), however, reveals that the methyl ester linkage of this inactive stereoisomer clashes sterically (at 1.2 Å) with the Cα atom of Gly142 (Fig. 3*f*). *R*-cocaine has been shown to inhibit hCE1 catalytic activity, with a $K_i$ of 0.01 mM, whereas *S*-cocaine is at least 1,000-fold less effective ($K_i$ >10 mM)[3].

hCE1 catalyzes the transesterification of cocaine with ethanol to generate cocaethylene[4]. During the two-step hydrolysis of cocaine, hCE1 forms a covalent acyl-enzyme intermediate at the carboxylic methyl ester position of cocaine, which is then attacked by ethanol to create cocaethylene (Fig. 1*a*). However, ethanol appears too large to access the acyl-enzyme intermediate through the top of the active site gorge, as it would have to pass by the bulky benzoyl and tropine rings of cocaine (Fig. 3*b*). We propose that ethanol accesses the active site of hCE1 through the side-door secondary pore adjacent to the large, flexible substrate-binding pocket (Fig. 3*b*). This allows direct access of ethanol to the covalent acyl-enzyme intermediate formed at Ser221. The entrance to the side-door secondary pore on the surface of hCE1 is lined by structurally flexible residues —

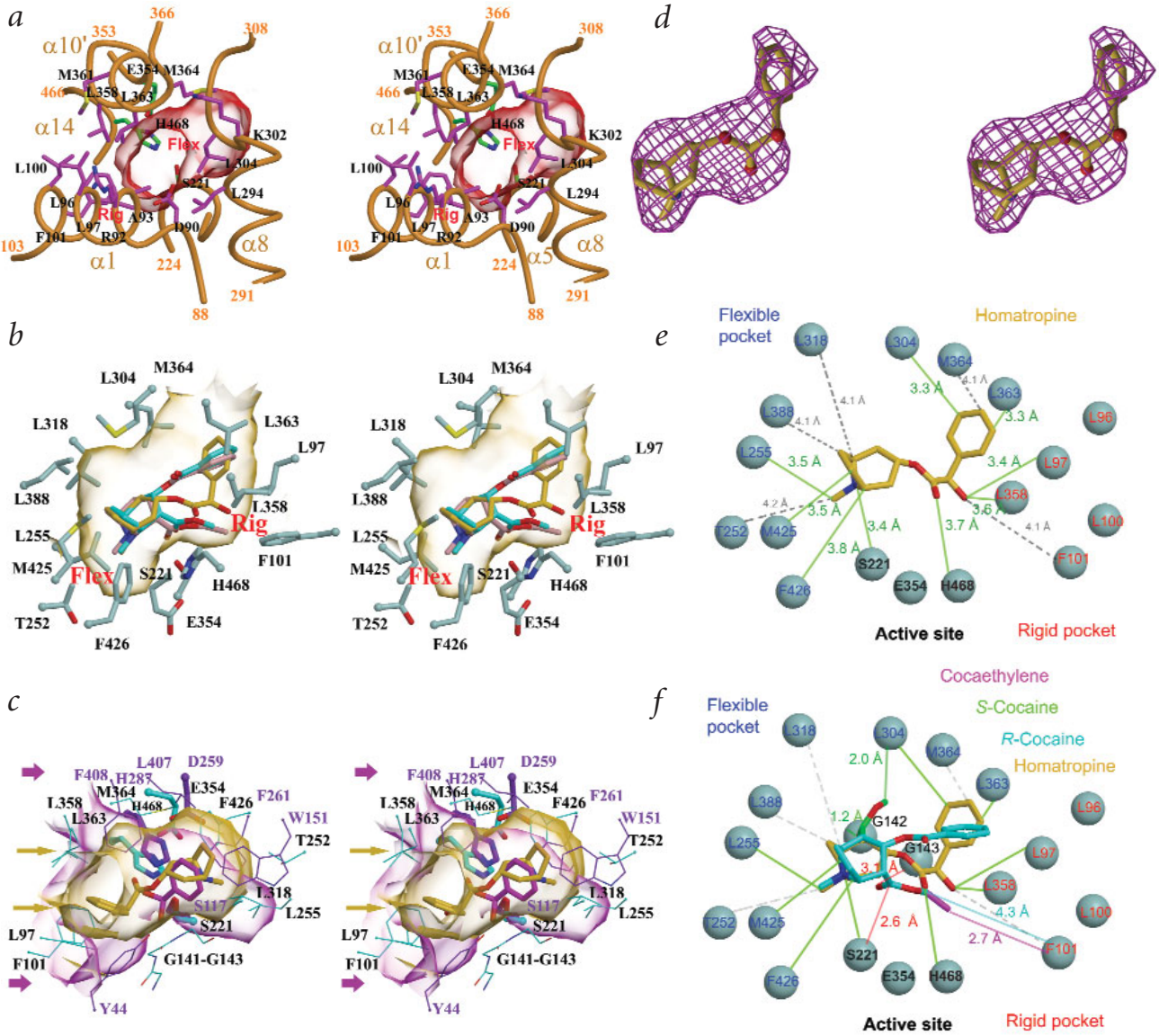


**Fig. 3** Cocaine metabolism by hCE1. ***a***, Stereo view of the entrance to the substrate-binding gorge of hCE1. The molecular surface of the hCE1 active site cavity is transparent red, with the active site residues green. The view in this image is roughly the same as in Fig. 2. ***b***, Stereo view of homatropine (gold) bound within the hCE1 catalytic pocket, along with a proposed binding mode for cocaine (cyan) and cocaethylene (pink). The molecular surface of the catalytic binding pocket is transparent gold. The catalytic Ser221 is located in between the large, flexible and small, rigid pockets (Flex and Rig, respectively). The molecule in this image has been rotated ~90° about the horizontal axis relative to that in Fig. 2. ***c***, Stereo view of the substrate-binding gorges of hCE1 and the bacterial cocE[22] viewed in roughly the same orientation as (*a*), rotated slightly about the *y*-axis. The molecular surfaces of the hCE1 (transparent gold) and cocE (transparent magenta) are shown. The catalytic triad (thick rendering) and the surrounding residues (thin) of hCE1 are in cyan; the catalytic triad (thick) and the surrounding residues (thin) of cocE are in purple. The homatropine (gold) and the phenyl boronic acid (magenta) are also shown. The entrances to the substrate-binding gorges of hCE1 and cocE are highlighted with gold and magenta arrows, respectively. ***d***, Stereo view of 2.8 Å resolution simulated annealing omit density contoured at 2.5 σ of homatropine bound at the active site of hCE1. ***e***, Schematic representation of the experimentally observed binding mode of the cocaine analog homatropine (gold) in the active site of hCE1. Average distances between amino acid side chains and atoms in homatropine are indicated with solid green lines (<4 Å) or dotted gray lines (>4 Å). ***f***, Schematic representation of the proposed binding modes of the active cocaine stereoisomer *R*-cocaine (cyan), the inactive stereoisomer *S*-cocaine (green) and the toxic metabolite cocaethylene (magenta) in the active site of hCE1. The position of the tropine ring of homatropine (gold) was used to dock *R*- and *S*-cocaine and cocaethylene. Note that only the methyl ester linkage of *S*-cocaine (green) is shown, and only the terminal methyl of the ethyl ester linkage of cocaethylene (magenta) is shown. The lines indicating the average distances between homatropine and hCE1 side chains remain in this figure, although the distances shown in (*e*) have been removed.

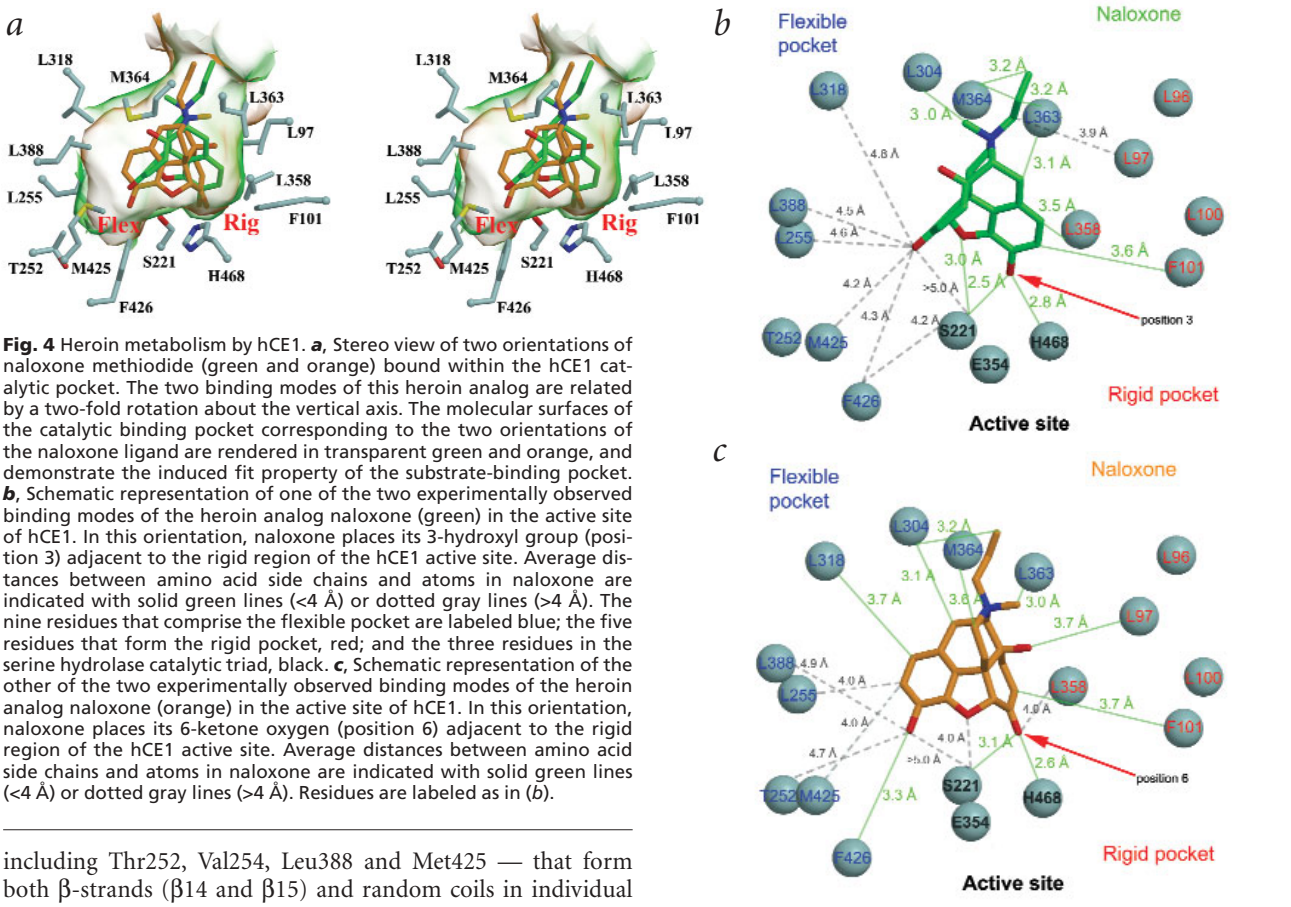


**Fig. 4** Heroin metabolism by hCE1. ***a***, Stereo view of two orientations of naloxone methiodide (green and orange) bound within the hCE1 catalytic pocket. The two binding modes of this heroin analog are related by a two-fold rotation about the vertical axis. The molecular surfaces of the catalytic binding pocket corresponding to the two orientations of the naloxone ligand are rendered in transparent green and orange, and demonstrate the induced fit property of the substrate-binding pocket. ***b***, Schematic representation of one of the two experimentally observed binding modes of the heroin analog naloxone (green) in the active site of hCE1. In this orientation, naloxone places its 3-hydroxyl group (position 3) adjacent to the rigid region of the hCE1 active site. Average distances between amino acid side chains and atoms in naloxone are indicated with solid green lines (<4 Å) or dotted gray lines (>4 Å). The nine residues that comprise the flexible pocket are labeled blue; the five residues that form the rigid pocket, red; and the three residues in the serine hydrolase catalytic triad, black. ***c***, Schematic representation of the other of the two experimentally observed binding modes of the heroin analog naloxone (orange) in the active site of hCE1. In this orientation, naloxone places its 6-ketone oxygen (position 6) adjacent to the rigid region of the hCE1 active site. Average distances between amino acid side chains and atoms in naloxone are indicated with solid green lines (<4 Å) or dotted gray lines (>4 Å). Residues are labeled as in (*b*).

including Thr252, Val254, Leu388 and Met425 — that form both β-strands (β14 and β15) and random coils in individual hCE1 monomers. This flexibility may facilitate the passage of small molecules like ethanol through the side door.

The human brain appears to contain only a C-terminally truncated form of hCE1 that lacks portions of the catalytic and regulatory domains central to creating the side door[19]. Cocaethylene cannot be formed in the brain, despite the ability of both ethanol and cocaine to enter this organ; cocaethylene is generated only in tissues such as liver, heart, and lung that contain hCE1 (refs. 20,21). Cocaethylene binds to hCE1 with reduced affinity ($K_i$ = 0.1 mM) relative to cocaine ($K_i$ = 0.01 mM)[3,4]. This difference in binding affinity appears to be due, in part, to the important role that the small, rigid pocket in the active site of hCE1 plays in substrate selectivity. The methyl ester linkage of cocaine fits well within this pocket (Fig. 3*b*,*f*). When cocaethylene is docked into the active site of hCE1, however, the terminal methyl on its ethyl ester group clashes sterically at 2.7 Å with the side chain of Phe101 in the rigid pocket of the enzyme (Fig. 3*b*,*f*). The reduction in binding affinity of cocaethylene for hCE1 may provide a molecular explanation for the extended serum half-life of cocaethylene relative to that of cocaine (100 min *versus* 64 min)[13].

We compared the hCE1–homatropine complex with the structure of a bacterial cocaine esterase (cocE)[22], which metabolizes the benzoyl ester group of cocaine (Fig. 1*a*). The entrance to the substrate-binding gorge of hCE1 is narrower compared with that of cocE (Fig. 3*c*). The two enzymes also orient cocaine in the opposite way within their active sites, as hCE1 places the tropine group of homatropine where cocE packs the benzoyl portion of cocaine. We further compared the hCE1–homatropine complex with the structure of a cocaine-binding antibody bound to *R*-cocaine[23] and found that the substrate binding characteristics of these proteins are different. In contrast to hCE1, the antibody packs hydrophobic side chains against the benzoyl and methyl groups of cocaine and contacts the tropine ring using hydrogen bonds. Thus, the substrate-binding gorge of hCE1 is unique with respect to other structures of cocaine-binding proteins reported thus far and may serve as an important model for understanding how cocaine binds to its psychoactive targets in human brain, including the dopamine transporter[3].

## Heroin metabolism by hCE1

The heroin analog naloxone methiodide was observed to bind in one orientation in 7 of the 12 monomers in the asymmetric unit of the hCE1–naloxone structure (green, Fig. 4*a*,*b*) and in an alternate orientation in the remaining 5 monomers (orange, Fig. 4*a*,*c*). The two naloxone-binding modes are related by an approximate two-fold rotation about the long axis of the ligand. The presence of two naloxone orientations suggests that hCE1 can metabolize the conversion of heroin to both 6-monoacetylmorphine and morphine. hCE1 is able to catalyze both reactions[3], but it is more efficient at the hydrolysis of heroin to 6-monoacetylmorphine (Fig. 4*a*, green), the first step of heroin metabolism[3]. Modeling heroin into the hCE1 active site provides a structural explanation for these biochemical observations. When heroin is positioned with the 3-acetyl group in the rigid pocket of hCE1 (Fig. 4*a*,*b*), the bridging ether oxygen of heroin is capable of receiving a hydrogen bond from Ser221, which may help to align the 3-acetyl linkage for catalysis.

## Substrate selectivity by hCE1

hCE1 has been proposed to recognize a large acyl moiety (held as the acyl-enzyme intermediate) and a small alcohol group (released as the alcohol product)[2,24]. This appears to be true for

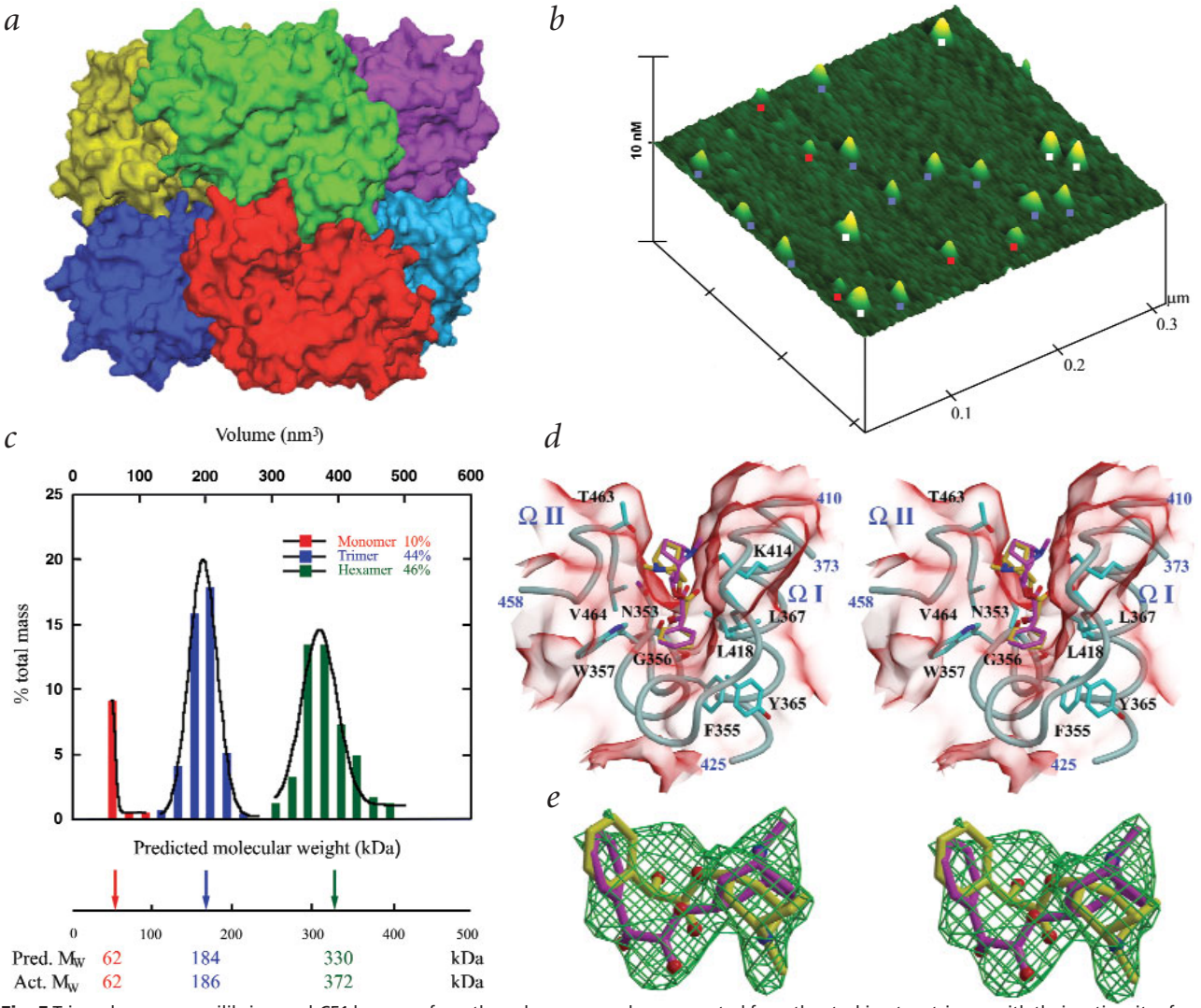


**Fig. 5** Trimer-hexamer equilibrium. ***a***, hCE1 hexamer from the naloxone complex, generated from the stacking two trimers with their active sites facing in. The upper trimer is rotated 90° about the horizontal axis relative to that in Fig. 2. The hexamer is viewed along the two-fold axis of rotation relating the green and red monomers. Note the Z-shaped interface formed between these individual protein molecules, as this region contains the Z site surface ligand-binding site. ***b***, Examination of the quaternary structure of hCE1 without ligand by AFM. This surface topography image shows a typical distribution of protein monomers (red squares), trimers (blue squares) and hexamers (white squares). ***c***, Graphical representation of 502 protein spots from 16 images of hCE1 without ligand generated by AFM analysis. The percent total mass, volume and predicted molecular weight are indicated. The volumetric estimation of predicted molecular weights (Pred. $M_w$) and actual molecular weights (Act. $M_w$) are shown in red for monomers, blue for trimers and green for hexamers. ***d***, Stereo view of the Z site surface ligand-binding pocket. The molecular surface of the red hCE1 monomer in (*a*) is rendered with transparency, with the Ω-loops that frame this binding site also shown in gray. Two stereoisomers of homatropine are shown in gold (*R*) and magenta (*S*), with the residues involved in homatropine binding in cyan. The homatropine complex contains two trimers, rather than a hexamer, in the asymmetric unit. The binding of homatropine to this surface-binding site appears to preclude the formation of a stacked hexamer created by the interdigitation of the Ω-loops. ***e***, Stereo view of 2.8 Å resolution simulated annealing omit density, contoured at 4.0 σ, of the two homatropine stereoisomers bound at the Z site of hCE1.

cocaine, in which benzoylecgonine serves as the large acyl moiety, and the methyl ester linkage is the small alcohol group. These classifications do not hold true for heroin, however, where the acyl group is the small acetyl linkage and the alcohol group is the large 6-monoacetylmorphine moiety. Indeed, we find that the acyl- and alcohol-binding pockets on the enzyme switch depending on which substrate is bound.

We define the pockets within the substrate-binding gorge of hCE1 as 'small, rigid' and 'large, flexible' (Figs. 3*a*,*b*,*e*,*f*, 4*a*–*c*). These definitions remain consistent with respect to the enzyme regardless of the substrate and help to explain how hCE1 acts on chemically divergent substrates like heroin and cocaine. hCE1 prefers methyl ester- or acetyl-type linkages within its small, rigid pocket and bulky groups within the large, flexible pocket. The larger pocket also appears to be conformable to accommodate different chemical structures, such as the tropine rings of cocaine and the tetracyclic morphine scaffold of heroin. Thus, the small, rigid pocket in hCE1 is selective, whereas its large, flexible pocket is promiscuous with regard to substrate specificity. Together, these pockets allow hCE1 to act on structurally distinct compounds containing either large or small alcohol substituent groups.

## Trimer-hexamer equilibrium

hCE1 was proposed to be a trimer on the basis of biochemical studies[3,4]. We find that hCE1 is indeed a C3 trimer in both the

**Table 1 Crystallographic statistics for hCE1 structures**

| | hCE1–naloxone | hCE1–homatropine |
|---|---|---|
| Resolution (Å)[1] | 30–2.9 (3.08–2.9) | 20–2.8 (2.87–2.8) |
| Space group | *P*1 | $P2_1$ |
| Asymmetric unit | Two hexamers | Two trimers |
| Cell constants | | |
| *a* (Å) | 91.2 | 55.4 |
| *b* (Å) | 120.7 | 178.8 |
| *c* (Å) | 177.0 | 199.6 |
| α (°) | 90.3 | 90 |
| β (°) | 89.3 | 90.2 |
| γ (°) | 99.2 | 90 |
| Reflections | | |
| Total | 285,255 | 292,059 |
| Unique | 157,959 | 82,155 |
| Mean redundancy | 1.8 | 3.6 |
| $R_{sym}$ (%)[1,2] | 9.2 (24.6) | 5.0 (11.4) |
| Wilson *B*-factor (Å$^2$) | 48.6 | 46.8 |
| Completeness (%)[1] | 96.3 (95.7) | 92.5 (80.6) |
| Mean I / σ [1] | 11.2 (2.4) | 11.1 (5.8) |
| $R_{cryst}$ (%)[1,3] | 21.4 (33.9) | 15.8 (25.1) |
| $R_{free}$ (%)[1,4] | 28.0 (41.8) | 22.2 (34.4) |
| Number of atoms | | |
| Protein | 49,570 | 24,768 |
| Solvent | 1,129 | 1,681 |
| Carbohydrate | 182 | 120 |
| Ligand | 240 | 240 |
| Ion | 0 | 2 |

[1]Number in parentheses is for the highest shell.
[2]$R_{sym} = \Sigma|I - \langle I\rangle| / \Sigma I$, where $I$ is the observed intensity and $\langle I\rangle$ is the average intensity of multiple symmetry-related observations of that reflection.
[3]$R_{cryst} = \Sigma||F_o| - |F_c|| / \Sigma|F_o|$, where $F_o$ and $F_c$ are the observed and calculated structure factors, respectively.
[4]$R_{free} = \Sigma||F_o| - |F_c|| / \Sigma|F_o|$ for 7% of the data not used at any stage of structural refinement.

homatropine- and naloxone-bound complexes. The trimer interface buries 475 Å$^2$ of solvent-accessible surface area and involves one salt bridge, two hydrogen bonds and one van der Waals contact between the αβ and catalytic domains of adjacent monomers (Fig. 2). *N*-linked glycosylation sites at Asn79 also appear to stabilize the trimer. In three of the six monomers in the homatropine complex, a sialic acid moiety from one monomer packs ~3 Å from the N terminus of α7 of an adjacent monomer within the trimer. Thus, these glycosylation sites, which have been demonstrated to be essential for the catalytic activity of the enzyme[25], contribute to the trimer interface of hCE1.

In the complex with naloxone, however, hCE1 forms an unexpected hexamer. Two hCE1 trimers stack with their substrate-binding gorges facing in, creating a hexamer with 32 point group symmetry (Fig. 5*a*). The resultant dimer interface is extensive, burying 1,900 Å$^2$ of solvent-accessible surface area on each monomer and involving 5 salt bridges, 11 hydrogen bonds and 5 van der Waals contacts. A significant portion of the dimer interface between hCE1 monomers is formed by the interdigitation of the Ω1 and Ω2 loops adjacent to the active site of the enzyme. The interdigitation of these loops creates a Z-shaped dimer interface (Fig. 5*a*); thus, we refer to this surface location as the 'Z site'.

Because this hexamer was not observed previously, we examined the oligomerization state of the enzyme using atomic force microscopy (AFM) in the absence of ligand and in the presence of 500-fold molar excess naloxone methiodide. AFM images reveal hCE1 monomers, trimers and hexamers (Fig. 5*b*). Volume analysis on 502 proteins spots from 16 AFM images of hCE1 alone reveals that 10% of the protein molecules exist as monomers, 44% form trimers and 46% form hexamers (Fig. 5*c*). Similarly, in the presence of 500-fold molar excess naloxone methiodide, 10% of the protein molecules are monomers, 40% form trimers and 50% form hexamers. Thus, crystallographic and AFM data reveal that hCE1 can exist in a trimer-hexamer equilibrium.

In the hCE1–homatropine complex, however, the asymmetric unit contains two unstacked hCE1 trimers. AFM analysis confirms that, in the presence of 100-fold molar excess homatropine, 9% of the hCE1 molecules remain monomers, 76% form trimers and only 15% form hexamers. Thus, the presence of homatropine shifts the hCE1 trimer-hexamer equilibrium toward trimer. The binding of homatropine to the Z site on the surface of hCE1 causes the shift in the trimer-hexamer equilibrium observed in the presence of this ligand. An enantiomeric mix of both *R*- and *S*-stereoisomers of homatropine was observed bound at the Z site (between the Ω loops) in each protein monomer in the hCE1–homatropine complex (Figs. 2, 5*d*,*e*). The binding of homatropine at this site prevents the packing of the two hCE1 trimers together to form a hexamer. This site is selective, however, as naloxone methiodide is unable to bind and effectively shift the oligomerization state of hCE1 from a hexamer to a trimer.

The guinea pig homolog of hCE1 (gpCE), which shares 71% sequence identity, was also shown to contain two substrate-binding sites per protein monomer[26]. The second substrate-binding site on gpCE is allosteric and contributes to positive cooperativity shown by the enzyme[26]. Thus, the second binding site on hCE1 is likely to enhance the catalytic activity of the enzyme with increasing substrate concentration and to control the trimer-hexamer equilibrium of the enzyme. The hCE1 hexamer may lend stability to the enzyme in circulating plasma, improving its ability to function as an efficient xenobiotic scavenger.

## Conclusion

The United States military is aggresively developing hCE1 as an organophosphate-hydrolase for prophylactic use before potential chemical weapons exposure[9–11]. In addition, the ability of hCE1 to bind to two cocaine molecules simultaneously and to generate the primary urinary metabolites of cocaine indicates that the enzyme has significant promise in the treatment of acute cocaine overdose. Other enzymes have been proposed for acute cocaine detoxification in humans but appear to have particular limitations[14,22]. For example, native hBuChE prefers the unnatural stereoisomer of cocaine (*S*-cocaine)[14], whereas the bacterial cocE shows a short half-life in circulation and may elicit immune reactions in humans[22]. The *N*-linked glycosylation sites of hCE1 and its trimer-hexamer equilibrium may enhance stability in circulating plasma, and the enzyme is not likely to generate the immune responses possible with non-native enzymes. Indeed, rhesus monkeys injected with an engineered tetrameric form of equine BuChE maintained both intact protein and BuChE activity with a half-life of 620 h, an improvement over monomeric and dimeric forms of the enzyme[27]. Purified hCE1 may be used to promote the clearance of cocaine in situations of acute overdose and may offer several days of protection against chemical warfare agents, such as sarin, soman, tabun and VX gas. Our crystal structures of hCE1 will enable the development of highly selective and efficient forms of the

enzyme for use in a variety of civilian and military settings. The engineering of novel hCE1 enzymes with improved catalytic power toward cocaine or organophosphate poisons is now in progress.

## Methods

**Crystallization.** A secreted, 62 kDa form of hCE1 was expressed using a baculovirus vector in *Spodoptera frugiperda* Sf21 cells and purified as described[28,29]. hCE1 was concentrated to 3 mg $ml^{-1}$ in 50 mM HEPES, pH 7.4, and crystallized in the presence of either 10 mM naloxone methiodide or 100 mM homatropine using sitting drop vapor diffusion at 22 °C. Crystals of 200–300 μm in size grew in 10% (w/v) PEG 3350, 0.4 M $Li_2SO_4$, 0.1 M NaCl, 0.1 M LiCl, 0.1 M citrate, pH 5.5, and 5% glycerol, and were cryo-protected in 15% (w/v) sucrose plus mother liquor before flash cooling in liquid nitrogen.

**Structure determination and refinement.** Diffraction data were collected at Stanford Synchrotron Radiation Laboratory (SSRL) beamline 9-1 and SER-CAT beamline 22-ID at the Advanced Photon Source (APS) at 100 K using cryo-cooled crystals, and were processed and reduced using MOSFLM[30] and HKL2000 (ref. 31). The hCE1–naloxone and hCE1–homatropine structures were determined by molecular replacement with AMoRe[32] using the structure of rCE (PDB entry 1K4Y)[16] as a search model (81% sequence identity). Residues 21–553 of the 566-amino acid enzyme were traced for each protein monomer. Structures were refined using torsion angle dynamics in CNS[33] with the maximum likelihood function target and included an overall anisotropic *B*-factor and a bulk solvent correction. Before any refinement, 7% of the observed data were set aside for crossvalidation using $R_{free}$. Noncrystallographic symmetry restraints were used for each structure at initial refinement stages and then removed so that each monomer was refined independently. Manual adjustments were performed using O[34] and $\sigma_A$[35]-weighted electron density maps. Simulated annealing omit and $\sigma_A$-weighted difference density maps were used to position ligands into clear density at the active site. *N*-linked glycosylation sites were traced in all complexes. In the homatropine complex, simulated annealing difference density of >4 σ frequently indicated the presence of an additional sialic acid sugar moiety located 4–7 Å from the first *N*-acetylglucosamines of the *N*-linked glycosylation sites at Asn79. These sialic acid sugars are not connected by clear density to the carbohydrate chain; however, they appear to stabilize the hCE1 trimer by packing against a neighboring protein monomer. In two of the six homatropine monomers, water molecules at the oxyanion holes were interpreted as chloride ions because of low thermal displacement parameters. In the two hexamers within the asymmetric unit of the naloxone structure, seven monomers indicated that one orientation of naloxone (green, Fig. 4*a*,*b*) satisfied the simulated annealing difference density maps, whereas in the other five monomers the second orientation (related by a 180° rotation relative to the first orientation; orange, Fig. 4*a*,*c*) appeared to fit well. In the homatropine complex, only one orientation of the ligand was observed at the active site, but two orientations were found to fit the electron density at the surface Z site. The six independent homatropine molecules bound at the active sites of hCE1 monomers share 0.72 Å r.m.s. deviation over all atoms. The tropine rings of homatropine, however, are more consistent in position and show an r.m.s. deviation of 0.16 Å. Final structures show good geometry with no Ramachandran outliers. Molecular graphic figures were created with MolScript[36], BobScript[37], Raster3D[38] and DINO (*www.dino3d.org*). Cocaine and cocaethylene were modeled into the hCE1 active site using the experimentally observed position of homatropine as a guide and were subsequently energy-minimized using CNS[33].

**Atomic force microscopy.** hCE1 at 25 nM was equilibrated at 37 °C for 15 min in 20 mM HEPES, pH 7.0, either alone or with 500-fold molar excess naloxone (12.5 μM) or 100-fold molar excess homatropine (2.5 μM). The enzyme was then diluted to 5 nM, deposited within 5 s onto freshly cleaved mica (Spruce Pine Mica), washed immediately with deionized distilled water and dried in a nitrogen gas stream. Imaging was performed in air on a Nanoscope IIIa (Digital Instrument) using Nanosensor Pointprobe non-contact/tapping mode sensors with 48 N $m^{-1}$ spring constants and 190 kHz resonance frequencies. Images were collected at a scan rate of 3.2 Hz and a scan size of 1 μm. Volume analysis using AFM data was performed using image plane fitting, image analysis and volume calculation as described[39].

**Coordinates.** Coordinates and structure factors have been deposited with the Protein Data Bank (accession codes 1MX5 and 1MX9 for the homatropine- and naloxone-bound complexes, respectively).

#### Acknowledgments

We thank G. Pielak, L. Spremulli, B. Bernstein and C. Kuhn for critical comments on the manuscript; P. Kuhn and J. Chrzas for help with data collection; D. Erie for access to AFM equipment; and members of the Redinbo Laboratory, including J. Chrencik, E. Howard-Williams, T. Lesher, S. Sakai and R. Watkins, for discussions and experimental assistance. The reseach was supported by the N.I.H. and a Burroughs Wellcome Career Award in the Biomedical Sciences (M.R.R), and by the N.I.H. (including a Core Grant) and the American Lebanese Syrian Associated Charities (P.M.P.).

#### Competing interests statement

The authors declare that they have no competing financial interests.

Received 24 February, 2003; accepted 14 March, 2003.

1. Satoh, T. & Hosokawa, M. The mammalian carboxylesterases: from molecules to functions. *Annu. Rev. Pharmacol. Toxicol.* **38**, 257–288 (1998).
2. Satoh, T. *et al.* Current progress on esterases: from molecular structure to function. *Drug Metab. Dispos.* **30**, 488–493 (2002).
3. Brzezinski, M.R. *et al.* Human liver carboxylesterase hCE-1: binding specificity for cocaine, heroin, and their metabolites and analogs. *Drug Metab. Dispos.* **25**, 1089–1096 (1997).
4. Brzezinski, M.R., Abraham, T.R., Stone, C.L., Dean, R.A. & Bosron, W.F. Purification and characterization of a human liver cocaine carboxylesterase that catalyzes the production of benzoylecgonine and the formation of cocaethylene from alcohol and cocaine. *Biochem. Pharmacol.* **48**, 1747–1755 (1994).
5. Tang, B.K. & Kalow, W. Variable activation of lovastatin by hydrolytic enzymes in human plasma and liver. *Eur. J. Clin. Pharmacol.* **47**, 449–451 (1995).
6. Alexson, S.E., Diczfalusy, M., Halldin, M. & Swedmark, S. Involvement of liver carboxylesterases in the *in vitro* metabolism of lidocaine. *Drug Metab. Dispos.* **30**, 643–647 (2002).
7. Takai, S. *et al.* Hydrolytic profile for ester- or amide-linkage by carboxylesterases pI 5.3 and 4.5 from human liver. *Biol. Pharm. Bull.* **20**, 869–873 (1997).
8. Ellgaard, L., Molinari, M. & Helenius, A. Setting the standards: quality control in the secretory pathway. *Science* **286**, 1882–1888 (1999).
9. Sweeney, R.E. & Maxwell, D.M. A theoretical model of the competition between hydrolase and carboxylesterase in protection against organophosphorus poisoning. *Math. Biosci.* **160**, 175–190 (1999).
10. Broomfield, C.A. & Kirby, S.D. Progress on the road to new nerve agent treatments. *J. Appl. Toxicol.* **21 Suppl. 1**, S43–S46 (2001).
11. Maxwell, D.M. & Brecht, K.M. Carboxylesterase: specificity and spontaneous reactivation of an endogenous scavenger for organophosphorus compounds. *J. Appl. Toxicol.* **21 Suppl. 1**, S103–S107 (2001).
12. Pindel, E.V. *et al.* Purification and cloning of a broad substrate specificity human liver carboxylesterase that catalyzes the hydrolysis of cocaine and heroin. *J. Biol. Chem.* **272**, 14769–14775 (1997).
13. Kamendulis, L.M., Brzezinski, M.R., Pindel, E.V., Bosron, W.F. & Dean, R.A. Metabolism of cocaine and heroin is catalyzed by the same human liver carboxylesterases. *J. Pharmacol. Exp. Ther.* **279**, 713–717 (1996).
14. Sun, H., Shen, M.L., Pang, Y.P., Lockridge, O. & Brimijoin, S. Re-engineering butyrylcholinesterase as a cocaine hydrolase. *J. Pharmacol. Exp. Ther.* **302**, 710–716 (2002).
15. Pennings, E.J., Leccese, A.P. & Wolff, F.A. Effects of concurrent use of alcohol and cocaine. *Addiction* **97**, 773–783 (2002).
16. Bencharit, S. *et al.* Structural insights into CPT-11 activation by mammalian carboxylesterases. *Nat. Struct. Biol.* **9**, 337–342 (2002).
17. Leszczynski, J.F. & Rose, G.D. Loops in globular proteins: a novel category of secondary structure. *Science* **234**, 849–855 (1986).
18. Kryger, G. *et al.* Structures of recombinant native and E202Q mutant human acetylcholinesterase complexed with the snake-venom toxin fasciculin-II. *Acta Crystallogr. D* **56**, 1385–1394 (2000).
19. Mori, M., Hosokawa, M., Ogasawara, Y., Tsukada, E. & Chiba, K. cDNA cloning, characterization and stable expression of novel human brain carboxylesterase. *FEBS Lett.* **458**, 17–22 (1999).
20. Dean, R.A., Zhang, J., Brzezinski, M.R. & Bosron, W.F. Tissue distribution of cocaine methyl esterase and ethyl transferase activities: correlation with carboxylesterase protein. *J. Pharmacol. Exp. Ther.* **275**, 965–971 (1995).
21. Kalasinsky, K.S. *et al.* Regional distribution of cocaine in postmortem brain of chronic human cocaine users. *J. Forensic Sci.* **45**, 1041–1048 (2000).
22. Larsen, N.A. *et al.* Crystal structure of a bacterial cocaine esterase. *Nat. Struct. Biol.* **9**, 17–21 (2002).
23. Larsen, N.A. *et al.* Crystal structure of a cocaine-binding antibody. *J. Mol. Biol.* **311**, 9–15 (2001).
24. Bosron, W.F. & Hurley, T.D. Lessons from a bacterial cocaine esterase. *Nat. Struct. Biol.* **9**, 4–5 (2002).
25. Kroetz, D.L., McBride, O.W. & Gonzalez, F.J. Glycosylation-dependent activity of baculovirus-expressed human liver carboxylesterases: cDNA cloning and characterization of two highly similar enzyme forms. *Biochemistry* **32**, 11606–11617 (1993).
26. Suzuki-Kurasaki, M., Yoshioka, T. & Uematsu, T. Purification and characterization of guinea-pig liver microsomal deacetylase involved in the deacetylation of the *O*-glucoside of *N*-hydroxyacetanilide. *Biochem. J.* **325**, 155–161 (1997).
27. Broomfield, C.A. *et al.* Protection by butyrylcholinesterase against organophosphorus poisoning in nonhuman primates. *J. Pharmacol. Exp. Ther.* **259**, 633–638 (1991).
28. Morton, C.L. & Potter, P.M. Comparison of *Escherichia coli*, *Saccharomyces cerevisiae*, *Pichia pastoris*, *Spodoptera frugiperda*, and COS7 cells for recombinant gene expression: application to a rabbit liver carboxylesterase. *Mol. Biotechnol.* **16**, 193–202 (2000).
29. Danks, M.K. *et al.* Comparison of activation of CPT-11 by rabbit and human carboxylesterases for use in enzyme/prodrug therapy. *Clin. Cancer Res.* **5**, 917–924 (1999).
30. Collaborative Computing Project, Number 4. The CCP4 suite: programs for protein crystallography. *Acta Crystallogr. D* **50**, 760–763 (1994).
31. Otwinowski, Z. & Minor, W. *Data collection and processing* (Daresbury Laboratories, Warrington; 1993).
32. Navaza, J. Implementation of molecular replacement in AMoRe. *Acta Crystallogr. D* **57**, 1367–1372 (2001).
33. Brunger, A.T. *et al.* Crystallography & NMR system: a new software suite for macromolecular structure determination. *Acta Crystallogr. D* **54**, 905–921 (1998).
34. Jones, T.A., Zou, J.Y., Cowan, S.W. & Kjeldgaard, M. Improved methods for building protein models in electron density maps and the location of errors in these models. *Acta Crystallogr. A* **47**, 110–119 (1991).
35. Read, R.J. Improved Fourier coefficients for maps using phases from partial structures with errors. *Acta Crystallogr. A* **42**, 140–149 (1986).
36. Kraulis, P.J. MOLSCRIPT: a program to produce both detailed and schematic plots of protein structures. *J. Appl. Crystallogr.* **24**, 946–950 (1991).
37. Esnouf, R.M. Further additions to MolScript version 1.4, including reading and contouring of electron-density maps. *Acta Crystallogr. D* **55**, 938–940 (1999).
38. Merritt, E.A. & Murphy, M.E.P. Raster3D version 2.0 — a program for photorealistic molecular graphics. *Acta Crystallogr. D* **50**, 869–873 (1991).
39. Ratcliff, G.C. & Erie, D.A. A novel single-molecule study to determine protein-protein association constants. *J. Am. Chem. Soc.* **123**, 5632–5635 (2001).

# Two crystal structures demonstrate large conformational changes in the eukaryotic ribosomal translocase

**Rene Jørgensen, Pedro A Ortiz, Anne Carr-Schmid, Poul Nissen, Terri Goss Kinzy & Gregers Rom Andersen**
*Nat. Struct. Biol.* **10,** 379–385 (2003).

Some of the amino acid residues in Figs. 2 and 3 of this paper were incorrectly labeled. In Fig. 2a, residue 535 should be a glutamate (E535); in Fig. 2d, residue 191 should be a threonine (T191) and residue 192 should be a tyrosine (Y192); and in Fig. 3a, residue 798 should be a phenylalanine (Phe798). The panels with corrected labels are printed here. The authors apologize for any inconvenience this may have caused.

**2a**

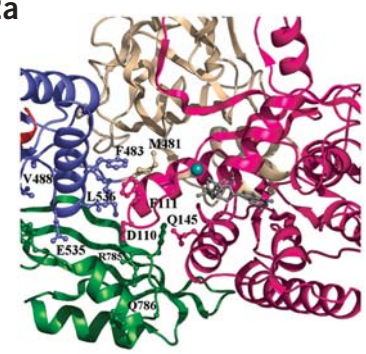


**2d**

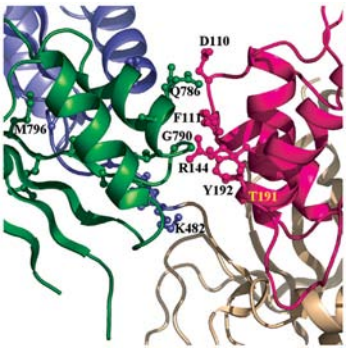


**3a**

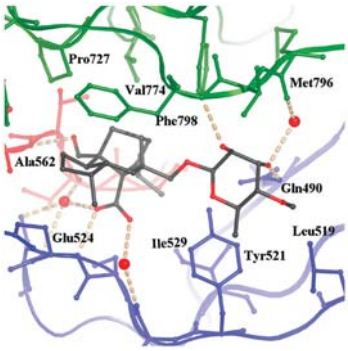


# Structural basis of heroin and cocaine metabolism by a promiscuous human drug-processing enzyme

**Sompop Bencharit, Christopher L Morton, Yu Xue, Philip M Potter & Matthew R Redinbo**
*Nat. Struct. Biol.* **10,** 349–356 (2003).

In the original print version of this manuscript, Fig. 1 contained several errors. In Fig. 1b, a double bond is missing in the structures of heroin, 6-acetylmorphine and morphine. In Fig. 1c, the *N*-alkyl group is one carbon too short in the naloxone methiodide structure. In addition, the stereochemistry of the structures in Fig. 1b and of naloxone methiodide in Fig. 1c was incorrect. The errors occurred during preparation of these panels for publication, and the authors apologize for any inconvenience this may have caused. Corrected versions of both panels are reproduced here.

**1b**

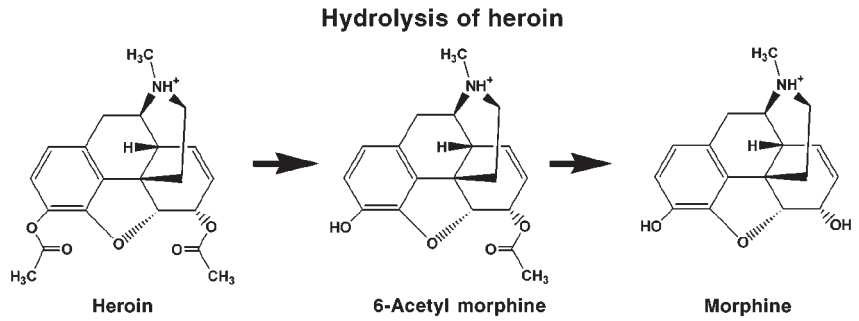


**1c**